Journal of Physics B: Atomic, Molecular and Optical Physics

Many-particle covalency, ionicity, and atomicity revisited for a few simple example molecules

OPEN ACCESS
IOP Publishing
Journal of Physics B: Atomic, Molecular and Optical Physics
J. Phys. B: At. Mol. Opt. Phys. **55** (2022) 185101 (13pp)
https://doi.org/10.1088/1361-6455/ac8298

Many-particle covalency, ionicity, and atomicity revisited for a few simple example molecules

Maciej Hendzel, Maciej Fidrysiak and Józef Spałek*

Institute of Theoretical Physics, Jagiellonian University, Łojasiewicza 11, PL-30-348 Kraków, Poland

E-mail: jozef.spalek@uj.edu.pl

Received 12 May 2022, revised 5 July 2022
Accepted for publication 19 July 2022
Published 19 August 2022

Abstract

We analyze two-particle binding factors of H_2, LiH, and HeH^+ molecules/ions with the help of our original exact diagonalization *ab initio* approach. The interelectronic correlations are taken into account rigorously within the second quantization scheme for restricted basis of renormalized single-particle wave functions, i.e., with their size readjusted in the correlated state. This allows us to determine the many-particle covalency and ionicity factors in a natural and intuitive manner in terms of the microscopic single-particle and interaction parameters, also determined within our method. We discuss the limitations of those basic characteristics and introduce the concept of atomicity, corresponding to the Mott and Hubbard criterion concerning localization threshold in many-particle systems. This addition introduces an atomic ingredient into the electron states and thus removes a spurious behavior of covalency with the increasing interatomic distance, as well as provides a more complete physical interpretation of bonding.

Keywords: atomicity in molecules, Mottness, resonant covalency, electron correlations, EDABI method

(Some figures may appear in colour only in the online journal)

1. Introduction

Determination of the microscopic nature of chemical bonding has been regarded as a problem of fundamental significance since the advent of quantum chemistry and solid state physics [1–3]. The qualitative classification of the valence-electrons state character as *covalent*, *ionic* or *atomic* helps to rationalize their overall features and select a detailed approach to analyze their detailed electronic properties. In this respect, the role of interactions and associated with them interelectronic correlations is crucial in discussing the evolution of bonding from either atomic or ionic character to predominantly covalent or band states of valence electrons. The many-electron approaches, such as configuration interaction (CI) [4] and others [5, 6], are particularly well suited for this task.

In this work we follow a different route and employ exact diagonalization *ab initio* (EDABI) method, combining the second-quantization formulation of quantum many-particle Hamiltonian with a concomitant readjustment of the single-particle wave functions in the correlated state of the system. This allows us to reinterpret some of the chemical bonding characteristics using concepts originating from condensed-matter physics, such as Mott–Hubbard localization. EDABI has been formulated in our group some time ago [7–9] and analyzed extensively in the context of correlated states in small clusters and one-dimensional solid-state systems. Apart from

* Author to whom any correspondence should be addressed.

providing rigorous description of selected properties, EDABI has supplied us with the evolution from the atomic- to a coherent-metallic state with decreasing interatomic distance. Also, modeling the metallization of molecular hydrogen solid has revealed a series of discontinuous first-order Mott-type transitions as a function of applied pressure [10–12]. The explicit question we would like to address here is to what extent the concepts essential extended to lattice quantum systems, such a *Mottness* [13, 14], may also be qualitatively applicable to finite molecular systems. Answering this question forced us to reanalyze the meaning of the two-particle covalency and related to it ionicity factors by starting from an analytic form of many-particle wave function. We suggest that such analysis may be useful in practical treatment of bonding, here carried out in two-atom–molecule situation, to make the discussion analytic and thus provide a degree of clarity.

The structure of the paper is as follows. In section 2 we summarize briefly the EDABI approach. In section 3 we reanalyze the bonding in H_2, HeH^+, and LiH systems. We also discuss there validity of the concept of atomicity—*Mottness*, with the help of which we single out the *resonant covalency* and atomicity factors. This discussion offers a resolution of the longstanding paradox of the increasing covalency with the increasing interatomic distance. Finally, in sections 4 and 5 we overview our approach. Formal details and tabulated values of the calculated microscopic parameters as a function of interatomic distance are provided in appendices A and B.

2. EDABI method and many-particle bonding

The EDABI method has been proposed by us and formulated in detail earlier [7, 9]. Below, we provide a brief summary of its main features, as this should by helpful in grasping the essence of our approach which will be needed in a subsequent interpretation of the results regarding many-particle covalency and ionicity, as well as the concept introduced by us of atomicity.

The starting point is the Hamiltonian containing all pairwise interactions in the second-quantized form is

$$\begin{aligned}\hat{\mathcal{H}} = {} & \epsilon_a \sum_{i} \hat{n}_{i\sigma} + {\sum_{ij\sigma}}' t_{ij}\, \hat{a}^{\dagger}_{i\sigma}\, \hat{a}_{j\sigma} + U \sum_{i} \hat{n}_{i\uparrow}\, \hat{n}_{i\downarrow} \\ & + \frac{1}{2} {\sum_{ij}}' K_{ij} \hat{n}_{i\sigma}\, \hat{n}_{j\sigma'} - \frac{1}{2} {\sum_{ij}}' J^{\mathrm{H}}_{ij} \left(\hat{\mathbf{S}}_i \cdot \hat{\mathbf{S}}_j - \frac{1}{4} \hat{n}_i \hat{n}_j \right) \\ & + \frac{1}{2} {\sum_{ij}}' J'_{ij} (\hat{a}^{\dagger}_{i\uparrow} \hat{a}^{\dagger}_{i\downarrow} \hat{a}_{j\downarrow} \hat{a}_{j\uparrow} + \mathrm{H.c.}) \\ & + \frac{1}{2} {\sum_{ij}}' V_{ij} (\hat{n}_{i\sigma} + \hat{n}_{j\sigma}) (\hat{a}^{\dagger}_{i\bar{\sigma}} \hat{a}_{j\bar{\sigma}} + \mathrm{H.c.}) + \mathcal{H}_{\mathrm{ion-ion}}, \quad (1)\end{aligned}$$

where H.c. denotes the Hermitian conjugation, $\hat{a}_{i\sigma}$ ($\hat{a}^{\dagger}_{i\sigma}$) are fermionic annihilation (creation) operators for state i and spin σ, $\hat{n}_{i\sigma} \equiv \hat{a}^{\dagger}_{i\sigma} \hat{a}_{i\sigma}$, and $\hat{n}_i \equiv \hat{n}_{i\uparrow} + \hat{n}_{i\downarrow} \equiv \hat{n}_{i\sigma} + \hat{n}_{i\bar{\sigma}}$. The spin operators are defined as $\hat{S}_i \equiv \frac{1}{2} \sum_{\alpha\beta} \hat{a}^{\dagger}_{i\alpha} \sigma_i^{\alpha\beta} \hat{a}_{i\beta}$ with σ_i representing Pauli matrices. The Hamiltonian contains the atomic and hopping parts ($\propto \epsilon_a$ and t_{ij}, respectively), the so-called Hubbard term $\propto U$; representing the intra-atomic interaction between the particles on the same atomic site i with opposite spins, the direct intersite Coulomb interaction $\propto K_{ij}$, Heisenberg exchange $\propto J^{\mathrm{H}}_{ij}$, and the two-particle and the correlated hopping terms ($\propto J'_{ij}$ and V_{ij}, respectively). The last term describes the ion–ion Coulomb interaction which is adopted here in its classical form.

We now proceed to definition of two-particle bonding in general situation and within the second-quantization representation. The N-particle state, $|\Psi_N\rangle$, may be expressed in terms of the N-particle wave function $\Psi(\mathbf{r}_1, \ldots, \mathbf{r}_N)$ and the corresponding field operators $\hat{\Psi}(\mathbf{r}_1), \ldots, \hat{\Psi}(\mathbf{r}_N)$ as

$$\begin{aligned}|\Psi_N\rangle = {} & \frac{1}{\sqrt{N!}} \int \mathrm{d}^3 r_1 \ldots \mathrm{d}^3 r_N\, \Psi_N(r_1, \ldots, r_N) \\ & \times \hat{\Psi}^{\dagger}_1(r_1) \ldots \hat{\Psi}^{\dagger}_N(r_N) |0\rangle, \quad (2)\end{aligned}$$

with $|0\rangle$ being the universal vacuum state in the Fock space (for pedagogical exposition see, e.g., [15]). Here we employ a short-hand notation $r_i \equiv (\mathbf{r}_i, \sigma_i)$, where $\sigma_i = \pm 1$ is the spin quantum number. We can revert this relation to determine the wave function $\Psi_N(r_1, \ldots, r_N)$, namely

$$\Psi_\alpha(r_1, \ldots, r_N) = \frac{1}{\sqrt{N!}} \langle 0 | \hat{\Psi}_1(r_1) \ldots \hat{\Psi}_N(r_N) | \lambda_\alpha \rangle, \quad (3)$$

where $|\lambda_\alpha\rangle$ is the eigenstate for which the wavefunction Ψ_α i explicitly determined. For spin-conserving interaction, $\alpha = (\sigma_1, \sigma_2, \ldots, \sigma_N)$ is fixed N-spin-configuration. In effect, we determine $|\lambda_\alpha\rangle$ states around ground eigenstate $|\lambda_\alpha\rangle \equiv |\lambda_{\min}\rangle$. Hamiltonian (1) is used to obtain the eigenstates which for two-electron H_2 system are discussed analytically in appendix A.

Since we focus explicitly on the two-site systems, the set of microscopic parameters (ϵ_a, t, U, K, J, J', and V) is defined through integrals of orthogonalized single particle basis functions, $\{w_i(\mathbf{r})\}$, used next to define the field operators in turn needed to construct the Hamiltonian (1). They are defined briefly first [7, 9], whereas the values of the microscopic parameters are defined in appendix B, starting from the nonorthogonal basis set of adjustable Slater functions. Namely, the orthogonalized atomic (Wannier) orbitals for H_2 molecule the $1s$ are defined via Slater orbitals $\{\psi_i(\mathbf{r})\}$ in the usual manner

$$w_{i\sigma}(\mathbf{r}) = \beta[\psi_{i\sigma}(\mathbf{r}) - \gamma \psi_{j\sigma}(\mathbf{r})], \quad (4)$$

where $\sigma \pm 1$ is spin quantum number $i \neq i = 1, 2$, and the coefficients β and γ take the form

$$\begin{cases} \beta = \dfrac{1}{\sqrt{2}} \sqrt{\dfrac{1 + \sqrt{1 - S^2}}{1 - S^2}}, \\ \gamma = \dfrac{S}{1 + \sqrt{1 - S^2}}, \end{cases} \quad (5)$$

so that $\beta^2 + \gamma^2 = 1$. The Slater orbitals $\psi_i(r) \equiv \sqrt{\frac{\alpha^3}{\pi}}\exp(-\alpha(\mathbf{r} - \mathbf{R}_i))$, with α being the inverse size of the orbital, are to be readjusted during the ground-state-energy minimization in *the correlated state*. Optimization over parameter α is motivated by the circumstance that the selected single-particle basis $\{\psi_i(\mathbf{r})\}$ is never complete in the quantum mechanical sense and thus such a procedure allows for a better estimate of the ground-state energy. This allows for the orbital-size adjustment in the interacting environment of remaining particles. In brief, the standard procedure of determining the quantum-mechanical state of the system is inverted in the sense that we first diagonalize many-particle Hamiltonian for fixed values of the microscopic parameters and, subsequently, readjust the wave function (inverse size, α^{-1}) in a recurrent fashion. The whole procedure is schematically illustrated by a flowchart composing figure 1.

The selected a single-particle basis for H_2 is composed of four orthogonalized wave functions with indices $i = 1, 2$ enumerating hydrogen atoms and $\sigma = \pm 1$ for each i. Thus, the truncated field operator takes the form

$$\hat{\Psi}(\mathbf{r}) = \sum_{i=1}^{2} w_i(\mathbf{r})\chi_\sigma(\mathbf{r})\hat{a}_{i\sigma}. \tag{6}$$

In that situation, the two-particle wave function is defined in accordance with equation (3), namely

$$\Psi_\alpha(\mathbf{r}_1, \mathbf{r}_2) = \frac{1}{\sqrt{2}}\langle 0|\hat{\Psi}_1(\mathbf{r}_1)\hat{\Psi}_2(\mathbf{r}_2)|\lambda_\alpha\rangle, \tag{7}$$

where $|\lambda_\alpha\rangle$ is the eigenstate (expressed in second quantization representation). Note that this method of approach allows to determine both the ground-state and the lowest excited states for a single optimal value of α.

Note that here the subscripts 1 and 2 of $\hat{\Psi}(\mathbf{r})$ contain both site and spin indices for brevity of notation. Parenthetically, one may generalize the above definition to the case of multiple (n) bonds (with $n \geqslant 1$) as

$$\Psi_{\mathrm{a}}(\mathbf{r}_1, \ldots, \mathbf{r}_{2n}) = \frac{1}{\sqrt{2n!}}\langle 0|\prod_{i=1}^{n}\hat{\Psi}_{\mathrm{i}}(\mathbf{r}_i)\prod_{j=n+1}^{2n}\hat{\Psi}_j(\mathbf{r}_j)|\lambda_\alpha^{(n)}\rangle. \tag{8}$$

In this manner the double ($n = 2$) and triple ($n = 3$) bonds can be defined, albeit numerically only and in more complex situations, e.g., in the case of carbon–carbon bonds. This scenario is not addressed here. Instead, we focus on the covalency and ionicity, as well as introduce *atomicity + covalency* factor, all for selected two-electron systems. However, we discuss first the inherent paradox of the increasing covalency with the increasing interatomic distance.

3. Covalency, ionicity, and atomicity on examples

3.1. Covalent bonding and ionicity in H_2 case

With the help of analysis presented in appendix A for the H_2 case, one can write down explicitly the two-electron wave function in the ground state for H_2 molecule ($n = 1$ case). The lowest-energy spin-singlet state is of the form

$$\Psi_0(\mathbf{r}_1, \mathbf{r}_2) = \frac{2(t+V)}{\sqrt{2D(D-U+K)}}\Psi_{\mathrm{c}}(\mathbf{r}_1, \mathbf{r}_2) - \frac{1}{2}\sqrt{\frac{D-U+K}{2D}}\Psi_{\mathrm{i}}(\mathbf{r}_1, \mathbf{r}_2), \tag{9}$$

where the covalent (Ψ_{c}) and ionic (Ψ_{i}) components, read

$$\Psi_{\mathrm{c}}(\mathbf{r}_1, \mathbf{r}_2) = [w_1(\mathbf{r}_1)w_2(\mathbf{r}_2) + w_1(\mathbf{r}_2)w_2(\mathbf{r}_1)] \times \left[\chi_\uparrow(\mathbf{r}_1)\chi_\downarrow(\mathbf{r}_2) - \chi_\downarrow(\mathbf{r}_1)\chi_\uparrow(\mathbf{r}_2)\right], \tag{10}$$

$$\Psi_{\mathrm{i}}(\mathbf{r}_1, \mathbf{r}_2) = [w_1(\mathbf{r}_1)w_1(\mathbf{r}_2) + w_2(\mathbf{r}_1)w_2(\mathbf{r}_2)] \times \left[\chi_\uparrow(\mathbf{r}_1)\chi_\downarrow(\mathbf{r}_2) - \chi_\downarrow(\mathbf{r}_1)\chi_\uparrow(\mathbf{r}_2)\right], \tag{11}$$

with

$$D \equiv \sqrt{(U-K)^2 + 16(t+V)^2}. \tag{12}$$

The ratio of the coefficients in (9) provides us with the relative ratio of covalency to ionicity in the ground-state spin-singlet configuration. The spin-singlet part is the same in both equations (10) and (11). Explicitly, the covalency and ionicity coefficients (factors) are defined as

$$\gamma_{\mathrm{c}} = \frac{16(t+V)^2}{16(t+V)^2 + (D-U+K)^2}, \tag{13}$$

and

$$\gamma_{\mathrm{i}} = \frac{(D-U+K)^2}{16(t+V)^2 + (D-U+K)^2}, \tag{14}$$

respectively, so that the condition $\gamma_{\mathrm{i}} + \gamma_{\mathrm{c}} = 1$ holds. The factor γ_{i} asymptotically approaches zero in the limit of large interatomic distance ($R \to \infty$), as expected. However, $\gamma_{\mathrm{c}} \to 1$ for $R \to \infty$ which represents an *unphysical* behavior [16–18]. This last feature will be discussed in detail below.

The obtained formulas are interpreted as follows. First, the coefficients γ_{c} and γ_{i} in the wave function (9) depend on all the interactions which are present in (1), i.e., they contain the effects electronic correlations. Second, the wave functions (10) and (11) take formally the Heitler–London form, but they are self-consistently optimized in the correlated state (their size α^{-1} is adjustable). Thus, the present formulation in its simplest from contains a semiquantitatively correct behavior in the large-R limit, as is demonstrated explicitly in figure 2.

In figure 2, we display the H_2 binding energy and have compared our EDABI calculated value with the results of CI and restricted Hartree–Fock (RHF) analysis. Note difference between the results for small $R < R_{\mathrm{bond}}$ (at minimum), as EDABI method provides slightly lower energies compared to those of full CI. This behavior should not influence the subsequent discussion in the large-R limit, which concerns us mainly here. Nonetheless, it is worth noting both CI and EDABI are variational approaches and perhaps our optimization of the wave-function size at small R is as important as the inclusion of the higher excited states. The binding energy is defined as $E_{\mathrm{bind}} = \lambda_5 - 2E_{\mathrm{H}}$ (λ_5 is defined in appendix A), where $E_{\mathrm{H}} = -1$ Ry is the energy of $1s$ state in atomic hydrogen. Next, we define the bonding and ionicity as the corresponding ratios of coefficients in equation (9), cf figure 3. We note

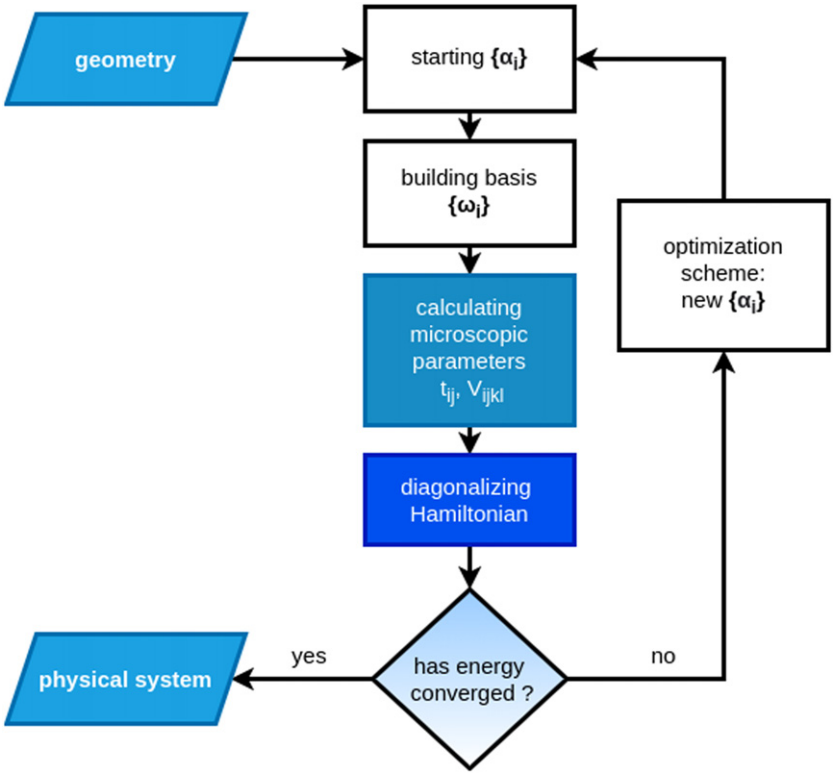

Figure 1. Flowchart of the EDABI method. The method is initialized by selection of a trial single-particle basis of wave functions, $\{w_i(\mathbf{r})\}$, and subsequent diagonalization the resulting many-particle Hamiltonian. Optimization of the single-particle states leads to an explicit determination of the trial-wavefunction parameters, microscopic interaction and hopping parameters, ground-state energy, and explicit many-particle wavefunction, all in the correlated interacting state. For detailed discussion see main text.

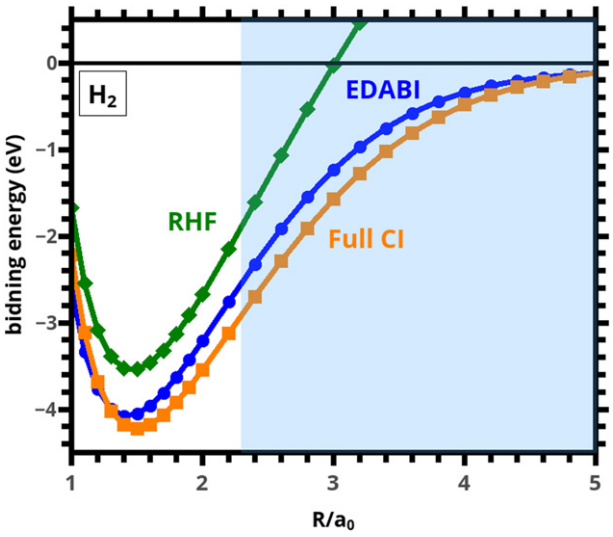

Figure 2. The H_2 binding energy versus relative interatomic distance, calculated within EDABI and compared with RHF and full CI method. a_0 is the Bohr radius. EDABI yields lightly lower energy than full CI calculation at very small interatomic distance, R; this difference does not alter the main point of our qualitative discussion.

that the covalency increases with the increasing interatomic distance at the expense of ionicity. However, this apparent inconsistency ignores the possibility of incipient atomicity of the *Mott–Hubbard type*, i.e., the tendency toward localization of electrons on parent atoms with increasing R (called briefly *the Mottness*). The Mott-type criterion for the localization of electron on H^+ ion (i.e., formation of renormalized atomic states) takes the form $2|t+V|/(U-K)=1$. This condition expresses the fact that the of bare kinetic energy is then equal to the effective repulsive Coulomb interaction $(U-K)$. In the strong correlation limit, the ratio is below unity, meaning this repulsive interaction becomes predominant (note that in the strict atomic limit, $t+V\equiv 0$ whereas $U-K=$ 1.25 Ry then). The regime of strong-correlations (Mottness) is marked explicitly in figures 3 and 4. It specifies a gradual evolution toward the atomic state. Namely, the shaded area should be regarded as the regime with steadily increasing atomicity of the electronic states with increasing R. Thus, the question of unphysically increased covalency for $R > R_{\mathrm{Mott}}$ is resolved in a natural manner as within the shaded area the covalency, γ_{c}, is composed of a sum of true (resonant) covalency $\bar{\gamma}_{\mathrm{c}} \to 0$ and atomicity $\gamma_{\mathrm{a}} \to 1$ as $R \to \infty$ (see the discussion below).

3.2. Correlation effects and incipient Mottness

The general meaning of the Mott (or Mott–Hubbard) effects is as follows. In condensed-matter physics the criterion takes the form of $U \simeq W$ [20], where $W \equiv |\sum_{j(i)} t_{ij}|$ is the bare bandwidth. The transition takes the form of often discontinuous metal–insulator transition for odd integer number of relevant valence electrons per atom. In molecular system, such as H_2, the HOMO–LUMO splitting $\simeq U-K$ must overcome the

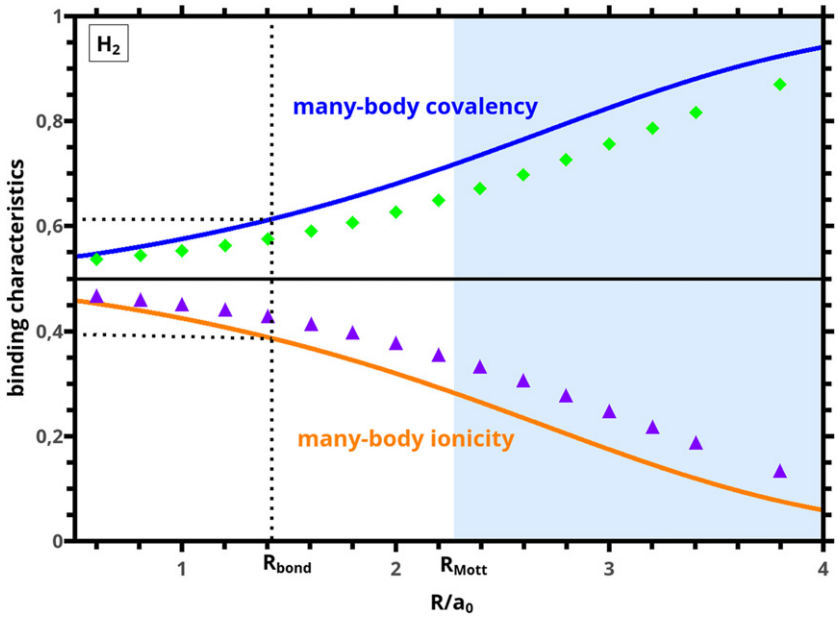

Figure 3. Two-particle covalency vs corresponding ionicity for H_2 molecule, calculated within EDABI method and compared with the results of reference [19]. Shaded regime marks a gradual evolution toward *atomicity*, as determined from the Mott–Hubbard criterion (see in the main text). Vertical dotted line marks equilibrium interatomic distance, whereas the horizontal dotted lines illustrate the dominant character of the covalency in that state (with the ratio $r = 1.43 \sim 2:1$)).

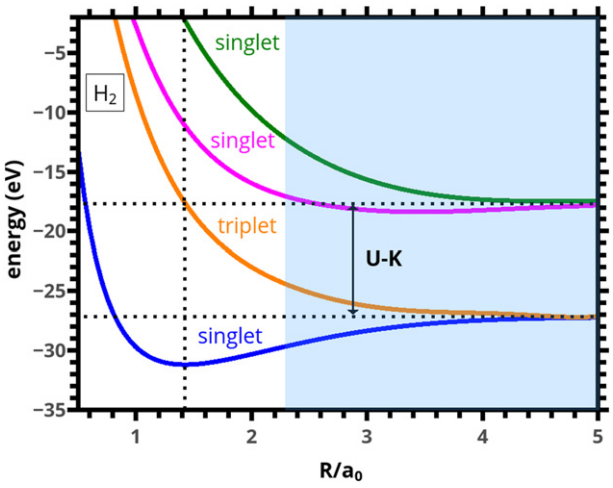

Figure 4. The lowest energy levels composed of three singlet and three triplet states, with the marked Mott regime and associated with it strong-correlation limit (shaded area). The scale $U - K$ represents the effective repulsive Coulomb interaction between electrons, i.e., the HOMO–LUMO splitting. The atomic character of the states increases with the increasing interatomic distance R.

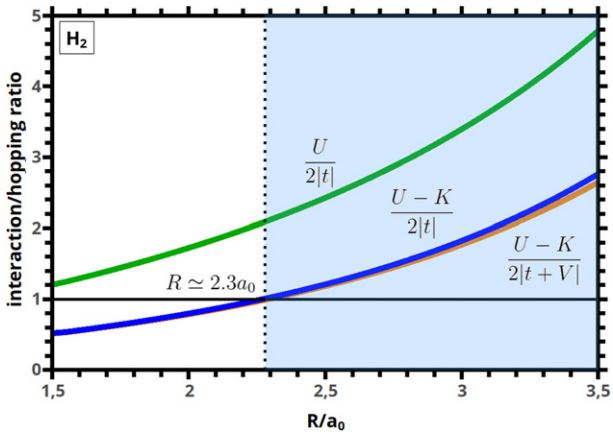

Figure 5. Characteristics of the H_2 state. The condition $(U - K)/(2|t + V|) = 1$ is the so-called Mott or Mott–Hubbard criterion for atomic localization which, in turn, determines the critical interatomic distance $R/a_0 \simeq 2.3$, representing the border of hatched area in figures 3 and 4. The atomic character of electron wave function becomes gradually enhanced with increasing $R > R_{\mathrm{Mott}}$. The remaining curves have a supplementary character (see main text).

effective interatomic hopping amplitude $W = 2|t|$. For Hamiltonian (1), the Mott–Hubbard criterion takes then the form $r \equiv (U - K)/(2|t + V|) \simeq 1$ so that both the correlated hopping and intersite Coulomb interaction contribute, in addition to t and U. In the present situation, the criterion separates only qualitatively the regime of strong correlations ($r \geqslant 1$) from that with moderate to weak correlations ($r < 1$). Various versions of the criterion have been shown in figure 5, depending on the theoretical model selected. Namely, the uppermost curve (in green) provides the criterion for the Hubbard model, which does not yield any Mottness point in the present situation. On the other hand, both the model with $V = 0$ and the full model (represented by the starting Hamiltonian (1)), are almost identical and yield the critical interatomic distance for localization $R = R_{\mathrm{Mott}} \simeq 2.3a_0$, i.e., well above the $R_{\mathrm{bond}} \simeq 1.43a_0$. Note also that even for equilibrium distance $R = R_{\mathrm{bond}}$ the hopping/interaction ratio is about $\sim$0.5, i.e., the electrons are moderately correlated.

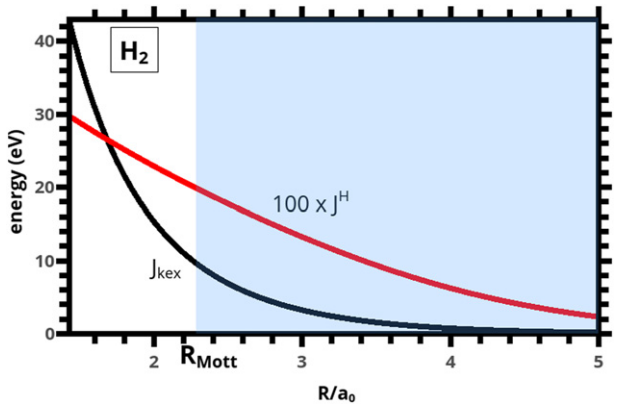

Figure 6. The antiferromagnetic kinetic exchange (superexchange) integral, $J_{\rm kex}$, calculated as a function of interatomic distance within EDABI approach. Superexchange dominates over its ferromagnetic Heisenberg correspondant, $J^{\rm H}$, and provides the justification for the molecule spin-singlet configuration. The kinetic exchange originates from virtual resonant hopping of the electron between the atoms [21].

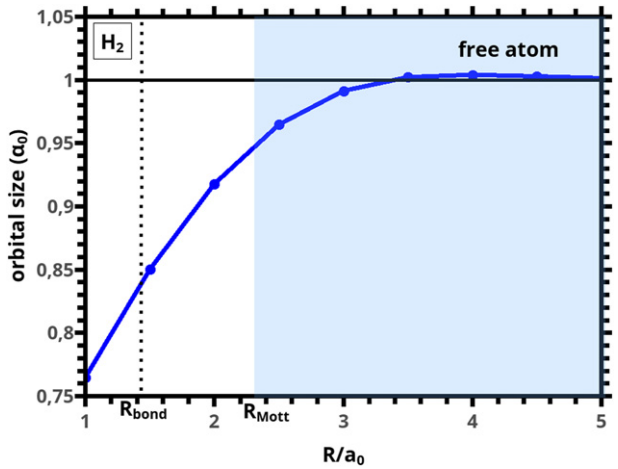

Figure 7. Renormalized $1s$ orbital size α^{-1} (in Bohr units a_0) vs relative interatomic distance for the H_2 molecule. Note that after crossing the Mott–Hubbard point $R = R_{\rm Mott}$, α^{-1} approaches rapidly its atomic-limit value $\alpha^{-1} = a_0$.

To complete the picture, we have also plotted in figure 6 the antiferromagnetic kinetic-exchange integral $J_{\rm kex} = 4(t+V)^2/(U-K)$ versus the direct (Heisenberg) ferromagnetic value $J^{\rm H}$, both as a function of relative distance R/a_0. The situation is that $J_{\rm kex} > J^{\rm H}$ for any distance R and this is the reason for the spin-singlet configuration of H_2 in the ground state. In brief, electrons hoping ('resonating') between the sites, possible only in the total spin-singlet state $|\lambda_5\rangle$, contribute essentially to the bonding.

To verify the conceptual validity of the introduced Mott threshold for atomicity onset, we have plotted in figure 7 the Slater-orbital size α^{-1} as a function of R. Upon crossing the threshold $R_{\rm Mott}$, α^{-1} indeed approaches rapidly with the further increasing R the $1s$ atomic size value $a_0 = 0.53$ Å. Instead, the main physical process contributing to the bonding are the virtual process between the sites. In effect, the ionicity and covalency factors lose their principal meaning for $R \gg 2.3$ Å.

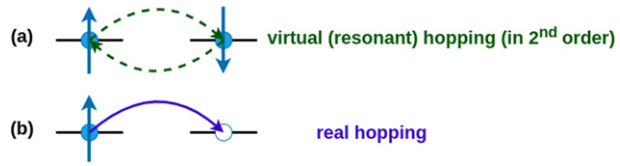

Figure 8. The virtual hopping processes that lead to the resonant covalency (a) and the real hopping, corresponding to the admixture of ionicity (b). For details see main text.

In conclusion, the dominant covalent character of H_2 molecule has a well defined meaning for $R \simeq R_{\rm bond}$, as it is twice as large as the corresponding ionicity factor. However, this decomposition loses gradually its principal meaning as R increases and crosses beyond $R_{\rm Mott} = 2.3a_0$. The ground state energy evolves slowly, but steadily toward, the atomic-limit value. Note also that the Hartree–Fock analysis (cf figure 2) provides unphysical results as this critical value of R is crossed. This means that, in the regime of large interatomic distance, the role of correlation becomes essential. In effect, our analysis is applicable then and can be systematically extended numerically by, e.g., enriching the single-particle basis. It would be also of general interest to ask if those concepts could be tested quantitatively by putting H_2 molecules on surfaces of other systems which would stretch the hydrogen-molecule size beyond the Mott–Hubbard threshold. Obviously, the analysis should then incorporate also the presence of the external surface potential of the substrate. However, this type of analysis goes beyond our goals here.

3.3. Physical reinterpretation of atomicity, covalency, and ionicity: resonant covalency

In order to provide a purely physical reinterpretation of covalency and ionicity we note that the form (3) of the covalent part contains sum of static products of the single-particle wave functions located on the sites 1 and 2 and their reverse; this is due to their indistinguishability in the quantum mechanical sense. On the contrary the coefficients $\gamma_{\rm c}$ and $\gamma_{\rm i}$ contain also virtual intersite processes depicted schematically in figure 8. In other words, the former factor contains a degree of atomicity in its static form, whereas the latter encompasses true dynamic virtual (hopping) processes of quantum-mechanical mixing. The question is how to separate those two factors into *atomicity* and *resonance covalency* parts in an analytic way.

To answer this dilemma we propose its following resolution. The allowed local (site) states are $|0,i\rangle$, $|\uparrow,i\rangle$, $|\downarrow,i\rangle$, and $|\downarrow,\uparrow,i\rangle$, i.e., the empty, single occupied with spin $\sigma = \uparrow$ or $\downarrow$, or the double atomic occupancies. Therefore, using the following identities

$$|0,i\rangle\langle 0,i| + \sum_{\sigma} |\sigma,i\rangle\langle\sigma,i| + |\uparrow,\downarrow,i\rangle\langle\uparrow,\downarrow,i| = \mathbb{I}, \qquad (15)$$

and its equivalent second-quantized from involving site occupancies

$$\langle(1-\hat{n}_{i\uparrow})(1-\hat{n}_{i\downarrow})\rangle + \langle\hat{n}_{i\uparrow}(1-\hat{n}_{i\downarrow})\rangle + \langle\hat{n}_{i\downarrow}(1-\hat{n}_{i\uparrow})\rangle + \langle\hat{n}_{i\uparrow}\hat{n}_{i\downarrow}\rangle = 1. \qquad (16)$$

Noting that the probability of empty atomic configuration is equal to that doubly occupied, i.e., physically corresponding to the electron–hole symmetry in condensed-matter systems, we obtain the formula for single-electron occupancy in the final form [22]

$$\nu \equiv \sum_{\sigma} \langle \hat{n}_{i\sigma}(1-\hat{n}_{i\bar{\sigma}})\rangle = 1 - 2d^2. \tag{17}$$

Explicitly, we propose to decompose single-occupancy probability ν in the following manner

$$\nu \equiv a + c = 1 - 2d^2, \tag{18}$$

where a is the atomicity, and c is called the *resonant (true) covalency*, and $d^2 \equiv \langle \hat{n}_{i\uparrow}\hat{n}_{i\downarrow}\rangle$ denotes atom double occupancy probability. Now, the resonant covalency describes the degree of mixing due to the virtual hopping admixture to the frozen (atomic) configuration (cf figure 8(a)). In the strong-correlation limit ($r > 1$), it can be defined as $c \equiv [|t+V|/(U-K)]^2$ and expresses the contribution of the processes (a) to the two-particle wave function in the second order [23, 24] as expressed by ratio of virtual (double hopping, forth and back) process to the Coulomb interaction change in the intermediate step. Therefore, the atomicity is evaluated as

$$a = \nu - c = 1 - 2d^2 - c. \tag{19}$$

In the equilibrium state of H_2, the resonant covalency reads $c \simeq 0.8$, whereas atomicity $a \simeq 0.1$ is practically negligible. Conversely, with increasing R, c decreases quite rapidly and approaches zero, whereas $a \to 1$, as anticipated.

Finally, in figure 9 we provide another characteristic containing atomicity, namely the R dependence d^2. This double occupancy probability can also characterize the ionicity. The last formula shows that the atomicity is complete when $d^2 = 0$ and then $\nu = a = 1$ (i.e., for $R \gg R_{\mathrm{Mott}}$). In the other words, the customarily, defined by (13) covalency, associated with the wave function (3), contains both atomicity and true covalency. For $R \gg R_{\mathrm{Mott}}$ it involves mainly atomicity with a small admixture of c and d^2. In this manner, the unphysical increase of γ_c with increasing R is resolved. In brief, fundamentally, we define the resonant (true) covalency c as proportional to the inverse Mottness, i.e.,

$$\text{true covalency} = 1/\text{Motness} \quad \text{or} \quad c \equiv 1/4r. \tag{20}$$

In conclusion, based on our analysis of H_2 molecule we suggest that the covalency definition through the values of γ_c is not conceptually precise, whereas the ionicity is properly accounted for either by γ_i or $2d^2$. Additionally, in this way the *redefined covalency* is complementary to the *Mottness* and vice versa.

3.4. LiH *and* HeH^+ *cases*

We now apply the concepts introduced above for H_2 molecule to the cases of LiH and HeH^+. In figures 10 and 11 we display the binding energies versus interatomic distance for HeH^+ molecular ion and LiH molecule, respectively. In the former case, the two $1s$ electrons are regarded as core electrons.

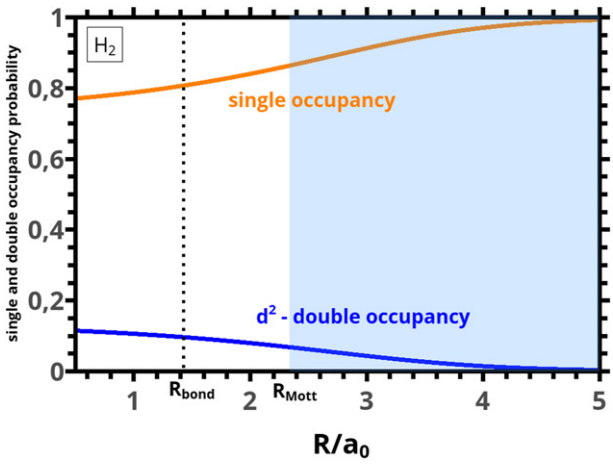

Figure 9. The atom double occupancy probability $d^2 \equiv \langle \hat{n}_{i\uparrow}\hat{n}_{i\downarrow}\rangle$ and simple occupancy ν, both vs R/a_0, calculated for H_2 molecule using EDABI approach. Note the presence of inflexion point at $R = R_{\mathrm{Mott}}$, signaling the onset of gradually increasing single occupancy (the orange curve). The single occupancy ν contains both resonant covalency and atomicity, which cannot be separated from each other at this stage. For detailed discussion see main text.

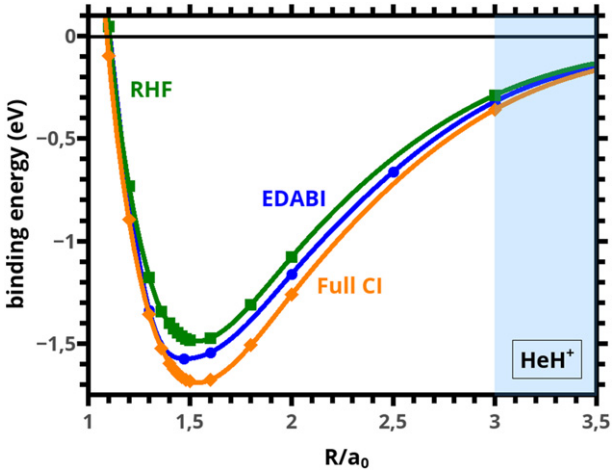

Figure 10. The HeH^+ binding energy versus relative interatomic distance, obtained using EDABI method and compared with RHF and full CI approach. a_0 is the Bohr radius.

Effectively, LiH is regarded as a molecule composed of one $2s$ electron due to Li and $1s$ electron due to H, with their orbitals adjustable when the interactions are included. Qualitatively, the character of these curves is similar to those of H_2, depicted in figure 2. The quantitative factors are different though and, in particular, the bond length is slightly larger than that in H_2 case.

To characterize further those two cases we have plotted in figures 12 and 13 the covalency and ionicity factors for those two systems, respectively. Note that for LiH the ionicity is predominant in a wide range of R, whereas the opposite is true for HeH^+. The difference arises from the circumstance that in LiH case the orbital size of $2s$ electron is decisively larger and has a higher energy leading to predominantly ionic configuration $\sim \mathrm{Li}^{+0.9}\mathrm{H}^{-0.9}$. In HeH^+, molecular ion the bonding is largely

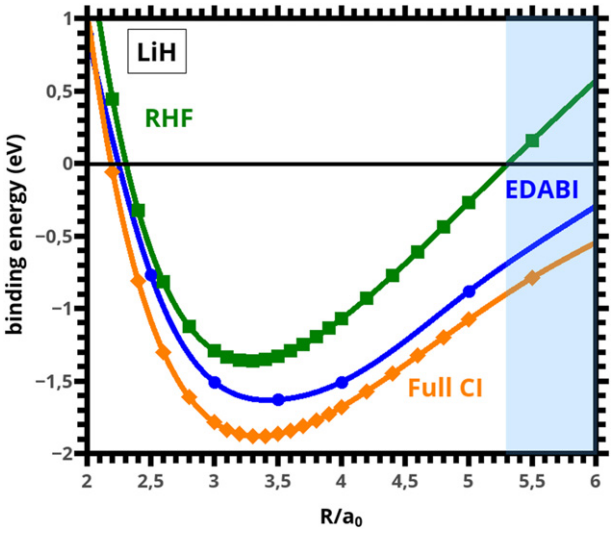

Figure 11. The LiH binding energy versus relative interatomic distance, obtained using EDABI method and compared with RHF and full CI approach. a_0 is the Bohr radius.

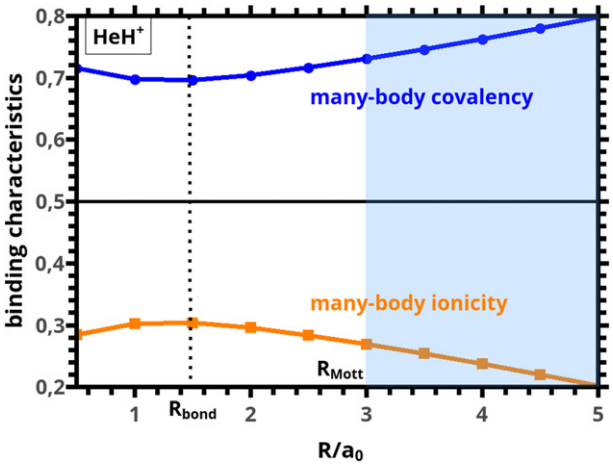

Figure 12. Many-body covalency vs many-body ionicity for HeH^+ molecule. The behavior is quite similar to that for H_2 molecule (cf figure 3).

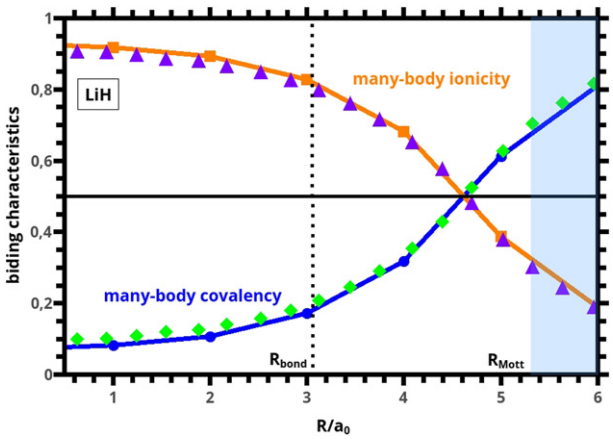

Figure 13. Many-body covalency vs many-body ionicity for LiH molecule. The points are taken from [19] for comparison. The covalency shows the same type of the unphysical R-dependence as in the case of H_2.

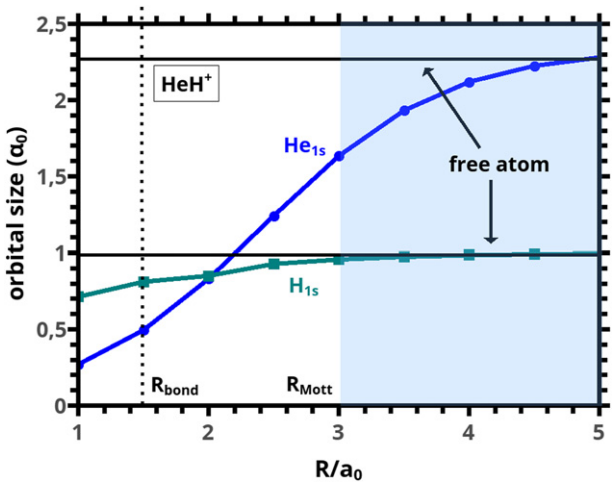

Figure 14. Atomic orbital size for He 1s and H 1s orbitals in HeH^+ molecular ion. Note that the Mott-type boundary has been drawn for the 1s states of He as this reached first upon increasing R.

covalent due to the fact that both two $1s^2$ He electrons hop (mix) with the H^+ state with no electrons in the corresponding 1s state.

One specific feature of those two systems should be noted, which is illustrated in figures 14 and 15, where the optimized sizes of the relevant orbitals has been shown. Namely, the size of 1s orbital of the He and 2s orbital of Li are strongly renormalized, the former largely expanded, whereas the latter contracted. The principal cause of this effect is the electronic correlation induced by the strong intraatomic (Hubbard) interaction $\sim U$. As this interaction in He is reduced by the flow of electron to the H^+ site, it is not so in the case of Li, where presence of the hydrogen electron strongly enhances the role of the interaction. In spite of those differences, both systems exhibit similar span of covalency regime. On the contrary, the incipient Mottness appears for larger distance R_{Mott} and this is presumably due to a larger renormalized-orbital size for Li. As can be seen from literature [25] and from our results here, HeH^+ is largely covalent and the whole analysis of a and c factors can be repeated here without any qualitative difference.

In table 1 we display the binding energies of the molecules H_2, HeH^+, LiH, regarded here as testing ground of our approach. For that reason we compare the obtained results with those deducted from other methods and with use of a richer single-particle basis. Even though our results are quantitatively not too accurate, they are obtained with simplest nontrivial basis, i.e., 1s states only for H_2 and HeH^+ cases, and with addition of 2s states on Li the LiH case. The EDABI results can be improved in a straightforward manner at the expense of computational resources. However in such a situation our following next discussion of bonding would be purely numerical. In other words, we accept the lower accurateness of E_{G} value within our method to allow for the analytic character of the subsequent discussion. One

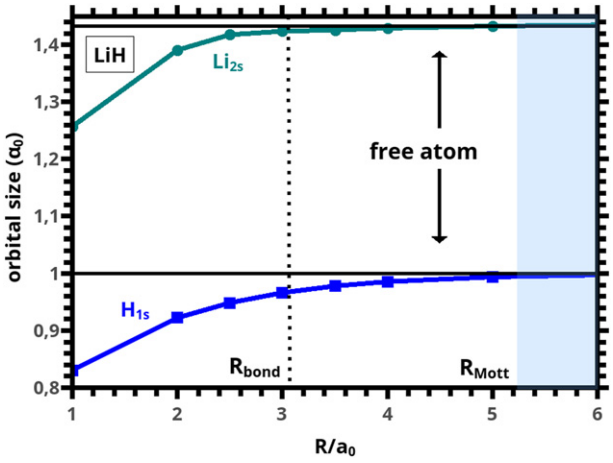

Figure 15. Atomic orbital size for H 1*s* and Li 2*s* orbitals in LiH molecule. Note the strong renormalization of atomic-orbital sizes, as well as a rapid convergence to the atomic values above $R = R_{\text{bond}}$, the latter being for the ionic bonding.

Table 1. Binding energy for H_2, HeH^+, and LiH molecules (in eV).

Method	H_2	HeH^+	LiH
EDABI	−4.0749	−1.5803	−1.6537
Full CI	−4.3824	−1.6849	−1.8846
RHF	−3.5963	−1.4839	−1.3616
Reference values	−4.3821[26]	−2.0542[27]	−1.3606[28]

can find more accurate value of ground state energy for HeH^+ [29].

4. Overall properties

We now compare results for those three model systems qualitatively. First, in figure 16 we plot relative contributions of the covalency and ionicity factors for the two-particle ground state (left), as well as a schematic size of the molecular orbitals relative to their original (atomic) size (right). The atomicity factor is not quantified at this stage. In the first two of them, the dynamics is solely due to 1*s* electrons, whereas in the LiH case the $1s^2$ configuration of electrons is frozen on Li and the whole dynamics is due to 1*s*–2*s* H–Li mixing and the corresponding interactions. This is the reason why LiH is largely ionic, whereas the remaining two are predominantly covalent, as illustrated in figure 13. One sees that the covalency in HeH^+ is larger than that for H_2 molecule, a rather unexpected intuitively result.

A separate discussion should be concerned with other overall properties of the systems studied. In table 2 the Mott (or Mott–Hubbard) critical distance R_{Mott} (in the units of a_0) is provided. This distance should be compared with the bond length R_{bond} calculated (cf table 3) according to three independent methods: EDABI, full CI, and RHF methods, respectively. We see that in each case R_{bond} is decisively lower than R_{Mott}. This means that the Mott-type boundary can be crossed only in the situation when the molecules are further apart, i.e., obtained artificially when, e.g., they are placed on surfaces

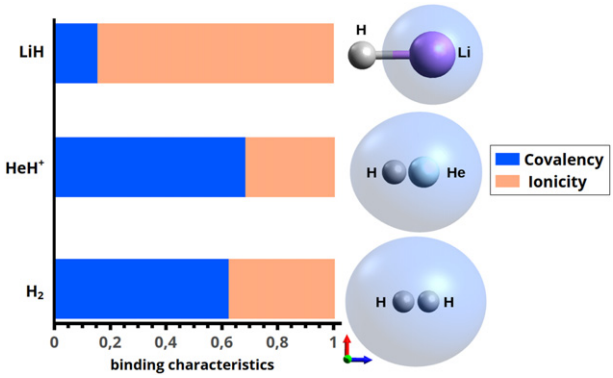

Figure 16. Schematic representation of the molecular orbitals for (isosurface probability density cut = 0.02) on the right, expressing relative covalency and ionicity contributions on the left.

Table 2. The interatomic distance corresponding to the Mott boundary regime calculated for H_2, HeH^+, and LiH molecules.

System	Mott boundary (a_0)
H_2	2.3
HeH^+	3.0
LiH	5.3

Table 3. Bond length for H_2, HeH^+, and LiH molecules (in units of a_0).>

Method	H_2	HeH^+	LiH
EDABI	1.430	1.469	3.382
Full CI	1.501	1.497	3.298
RHF	1.450	1.493	3.208
Reference values	1.398 [26]	1.463 [27]	3.015 [28]

with an external force elongating them. Particularly favorable situation occurs when molecules are placed in the environment with a large dielectric constant, as then interaction weakens and the bond length increases. Clearly, then the whole analysis must be revised and a realistic configuration with inclusion of appropriate external (surface) potential. We believe that the essential features of our analysis should survive when the molecule is placed in such environment, i.e., in a potential stretching equally both atoms.

In table 1 the binding energies are listed and compared with those from other methods. These numerical results present probably the weakest point of our EDABI method, since the corresponding values obtained are not very accurate. Nevertheless, we do not consider our method as a practical computing tool. Instead our main aim here was to extend, albeit at best in a semiquantitative manner, the basis for multi-electron covalency and ionicity, enriched by the concept of atomicity, all induced by the electronic correlations. Obviously, the approach can be extended in a straightforward manner by enlarging the single-particle basis and applied for the systems with larger atoms. Both of these factors have been considered by us before [7, 9] for model systems, with one limitation, that we have not analyzed there the bonding properties. This

Table 4. Calculated EDABI values of the equilibrium parameters for LiH, HeH^+, and H_2 molecules.

Parameter	LiH	H_2	HeH^+
E_G (eV)	−217.45	−31.198	−79.675
U_{1sLi} (eV)	49.062	N/A	N/A
U_{1sH} (eV)	18.559	22.490	19.592
U_{1sHe} (eV)	N/A	N/A	14.925
U_{2sLi} (eV)	12.784	N/A	N/A
t (eV)	−21.150	−9.9049	−15.674
K (eV)	14.368	13.007	11.374
α_{1sH} (a_0^{-1})	1.035	1.194	1.240
α_{1sHe} (a_0^{-1})	N/A	N/A	2.095
α_{2sLi} (a_0^{-1})	1.329	N/A	N/A

analysis should be explored further along the lines discussed here.

Finally, in table 4 we list the most important microscopic parameters in the equilibrium state. A more detailed analysis of those is presented in appendix B. The values of Coulomb-interaction parameters will be reduced by the dielectric constant factor if system under consideration is placed on surface of an insulating material. This should rescale all the parameter values accordingly.

5. Outlook

The reason for selecting the three systems analyzed here is caused by the circumstance that HeH^+ is strongly covalent, LiH strongly ionic, and H_2 can be placed in between them. On example of the last of them our novel concept of atomicity and resonant covalency have been proposed.

The introduced here atomicity for the case of molecular system (corresponding to Mott–Hubbard localization effects in periodic systems) amounts to specifying a gradual transformation from molecular to atomic language in describing their electronic states, as a function of interatomic distance. This changeover is the basic feature and is associated with the essential change in regarding those particles as evolving within *indistinguishable* (molecular) character and acquiring eventually the form of *distinguishable* (atomic) states.

One must also underline that the concept of atomicity here is quantitative in nature. This is because the Mott–Hubbard localization concept in condensed-matter systems [13, 20] appears usually as a first-order transition, requiring the energy equality of the two macro configuration (delocalized, localized) at this phase transition. Here the evolution may be regarded as a supercritical behavior at best [13, 30, 31]. However, the antiferromagnetic kinetic exchange survives even when the states are becoming orbitally distinguishable [32].

Certainly, a further insight is required to quantify the present discussion for more complex systems. The present concepts are proposed to clarify the obviously *unphysical behavior* of the increasing covalency with the increasing interatomic distance. As far as we are aware of, this inconsistency, although intuitively understandable, has not been discussed explicitly in the quantum-chemical literature. Also, the emerging atomicity here squares well with the Mott's original argument [20] that the metallic (covalent) state of electrons in a periodic system is ruled out at (semi)macroscopic interatomic distances.

Acknowledgments

This work was supported by Grants OPUS Nos. UMO-2018/29/B/ST3/02646 and UMO-2021/41/B/ST3/04070 from Narodowe Centrum Nauki. We would like to thank Prof. Ewa Brocławik and Dr Mariusz Radoń for discussions and criticism. We are also grateful to Andrzej Biborski and Andrzej P Kadzielawa for making available to us their QMT library.

Data availability statement

All data that support the findings of this study are included within the article (and any supplementary files).

Appendix A. Eigenvalues and eigenstates for H_2 molecule

Starting from the orthogonalized restricted basis, we define the field operators as

$$\hat{\psi}_\sigma(\mathbf{r}) = w_1(\mathbf{r})\chi_\sigma(1)\hat{a}_{1\sigma} + w_2(\mathbf{r})\chi_\sigma(2)\hat{a}_{2\sigma}, \tag{A.1}$$

$$\hat{\psi}^\dagger_\sigma(\mathbf{r}) = w^*_1(\mathbf{r})\chi_\sigma(1)\hat{a}^\dagger_{1\sigma} + w^*_2(\mathbf{r})\chi_\sigma(2)\hat{a}^\dagger_{2\sigma}, \tag{A.2}$$

or, in compact notation, as

$$\hat{\psi}(\mathbf{r}) \equiv \begin{pmatrix} \hat{\psi}_\uparrow(\mathbf{r}) \\ \hat{\psi}_\downarrow(\mathbf{r}) \end{pmatrix}. \tag{A.3}$$

In the above, $\hat{a}_{i\sigma}$ and $\hat{a}^\dagger_{i\sigma}$ are electron annihilation and creation operators in the state $w_{i\sigma}(\mathbf{r}) \equiv w_1(\mathbf{r})\chi_\sigma(1)$. Also, as we restrict here to s-orbital systems, the molecular (Wannier) functions can be taken as real if the condition $J' = J^H$ holds. Using the representation (A.3), we obtain Hamiltonian (1) with the microscopic parameters expressed through the Slater orbitals and coefficients β and γ (cf equation (5)), or explicitly through inverse orbital size α and interatomic distance R (see e.g. [7, 9]). The relevant physical quantities may be thus obtained as a function of R, with the orbital parameter α optimized in each case.

To obtain the ground state energy E_G for fixed R, the Hamiltonian (1) is diagonalized. This is carried out by making use of the global symmetry respecting two-particle states, leading to block-diagonal many-body Hilbert space, with specified values of the total spin, S, and its z-component, S^z, as well with transposition antisymmetry preserved. In effect, one can start

Table B1. Ground state energy and microscopic parameters for H_2 molecule (in eV).

R (a_0)	E_G/N	ϵ	t	U	K	J	V
0.5	−657	−14.29	−31.75	30.06	19.43	0.43	−0.28
1	−1486	−22.51	−15.95	25.29	15.43	0.36	−0.19
1.5	−1558	−23.84	−9.21	22.08	12.67	0.29	−0.16
2	−1516	−23.41	−5.79	19.96	10.75	0.23	−0.16
2.5	−1461	−22.56	−3.84	18.61	9.34	0.18	−0.16
3	−1418	−21.67	−2.62	17.81	8.24	0.13	−0.16
3.5	−1389	−20.86	−1.82	17.38	7.35	0.09	−0.16
4	−1373	−20.15	−1.26	17.18	6.60	0.06	−0.15
4.5	−1365	−19.52	−0.86	17.09	5.95	0.04	−0.14
5	−1362	−18.98	−0.59	17.05	5.40	0.02	−0.12

the basis of $\binom{4}{2} = 6$ following states

$$\begin{cases} |1\rangle = \hat{a}^\dagger_{1\uparrow}\hat{a}^\dagger_{2\uparrow}|0\rangle, \\ |2\rangle = \hat{a}^\dagger_{1\downarrow}\hat{a}^\dagger_{2\downarrow}|0\rangle, \\ |3\rangle = \frac{1}{\sqrt{2}}(\hat{a}^\dagger_{1\uparrow}\hat{a}^\dagger_{2\downarrow} + \hat{a}^\dagger_{1\downarrow}\hat{a}^\dagger_{2\uparrow})|0\rangle, \\ |4\rangle = \frac{1}{\sqrt{2}}(\hat{a}^\dagger_{1\uparrow}\hat{a}^\dagger_{2\downarrow} - \hat{a}^\dagger_{1\downarrow}\hat{a}^\dagger_{2\uparrow})|0\rangle, \\ |5\rangle = \frac{1}{\sqrt{2}}(\hat{a}^\dagger_{1\uparrow}\hat{a}^\dagger_{1\downarrow} + \hat{a}^\dagger_{2\downarrow}\hat{a}^\dagger_{2\uparrow})|0\rangle, \\ |6\rangle = \frac{1}{\sqrt{2}}(\hat{a}^\dagger_{1\uparrow}\hat{a}^\dagger_{1\downarrow} - \hat{a}^\dagger_{2\downarrow}\hat{a}^\dagger_{2\uparrow})|0\rangle. \end{cases} \tag{A.4}$$

The first three are the spin-triplet states with $S^z = +1, -1, 0$, whereas the next three are inter- and intra-site singlets, respectively. The triplet state does not hybridize with other states and provides three 1×1 irreducible blocks with eigenvalues $\lambda_1 = \lambda_2 = \lambda_3 = \epsilon_1 + \epsilon_2 + K - J^H$. The remaining three singlet states compose the 3×3 block, so the Hamiltonian in that Fock subspace takes the form

$$\hat{\mathcal{H}} = \begin{pmatrix} \epsilon + K + J^H & 2(t+V) & 0 \\ 2(t+V) & 2\epsilon + J + U & \frac{1}{2}(U_1 - U_2) \\ 0 & \frac{1}{2}(U_1 - U_2) & 2\epsilon + U - J^H \end{pmatrix}, \tag{A.5}$$

where $\epsilon \equiv (\epsilon_1 + \epsilon_2)/2$ and $U \equiv (U_1 + U_2)/2$. This formulation allows to apply this formalism to both H_2 (where $U_1 = U_2 = U$ and $\epsilon_1 + \epsilon_2 = \epsilon$), and to HeH^+ and LiH, where those simplifications are not met due to inequivalent atoms involved.

In the case of H_2, the eigenvalues of equation (A.5) take the form

$$\lambda_{4,5} = 2\epsilon + \frac{1}{2}(K+U) + J \pm \frac{1}{2}D, \tag{A.6}$$

$$\lambda_6 = 2\epsilon + U - J, \tag{A.7}$$

with $D \equiv [(U-K)^2 + 16(t+V)^2]^{\frac{1}{2}}$. The corresponding eigenstates are

$$|\lambda_{4,5}\rangle \equiv |\lambda_\pm\rangle = \frac{1}{[D(D \pm U \mp K)]^{\frac{1}{2}}}[(4(t+V))|4\rangle \pm (D \pm U \mp K)|5\rangle], \tag{A.8}$$

where, for simplicity, we have defined the atomic-limit energy as the reference point, $\epsilon = 0$. We note that the eigenstates $|\lambda_{4,5}\rangle$ are superposed of the symmetric ionic state $|5\rangle$ and covalent part $|4\rangle$. The state $|\lambda_5\rangle$ is the ground state as the λ_5 eigenvalue is the lowest one. In the limit $U \gg |t+V|$, the λ_5 eigenvalue reads

$$\lambda_5 \simeq 2\epsilon + J^H + K - \frac{4(t+V)^2}{U-K}. \tag{A.9}$$

The last term on the right-hand side of equation (A.9) is the so-called kinetic-exchange contribution. It competes with ferromagnetic Heisenberg exchange $\sim J^H$. In similar manner, the two-particle states for HeH^+ and LiH are obtained, except that in those two cases, the diagonalization of the Hamiltonian matrix (A.5) cannot be carried out analytically, since the $\epsilon_1 \neq \epsilon_2$ and $U_1 \neq U_2$. The singlet state $|\lambda_5\rangle$ is elaborated further throughout the main text.

Appendix B. Tables of relevant quantities and parameters for considered systems

In tables B1–B3 we provide relevant quantities and microscopic parameters versus R, obtained within EDABI scheme for the three systems discussed in main text, i.e., H_2, HeH^+, and LiH.

Note that the value of $|t|$ is comparable to U in the limit $R < R_{bond}$ and diminishes spectacularly when $R > R_{bond}$ (i.e. in the strong-correlation regime).

The RHF and CI computations were carried out using the GAMESS code and the 6–31 G basis set to represent the Slater functions. Numerical accuracy for the EDABI calculations is $10^{-4}\ a_0$ for R and 10^{-5} eV for energy, respectively.

Table B2. Ground state energy and microscopic parameters for HeH^+ molecular ion (in eV).

$R\ (a_0)$	E_G/N	ϵ_H	ϵ_{He}	t	U_H	U_{He}	K	V
0.5	−27.84	−22.42	−14.32	−24.07	22.35	36.70	11.17	−0.99
1	−38.54	−32.81	−32.43	−18.96	20.57	21.85	8.48	−0.75
1.5	−39.84	−34.59	−33.13	−15.49	19.54	14.62	6.72	−0.60
2	−39.63	−34.10	−29.57	−13.15	18.95	11.10	5.66	−0.50
2.5	−39.38	−32.20	−25.93	−11.55	18.61	9.39	4.95	−0.44
3	−39.21	−29.67	−22.86	−10.38	18.41	8.56	4.54	−0.39
3.5	−37.68	−27.20	−20.45	−9.45	18.30	8.15	4.26	−0.36
4	−39.09	−25.08	−18.62	−8.64	18.23	7.96	4.05	−0.33
4.5	−38.97	−23.37	−17.23	−7.90	18.19	7.86	3.86	−0.31
5	−38.92	−22.01	−16.16	−7.20	18.17	7.82	3.69	−0.31

Table B3. Ground state energy and microscopic parameters for LiH molecule (in eV).

$R\ (a_0)$	E_G/N	ϵ_H	ϵ_{2sLi}	t	U_H	U_{2sLi}	K	V
1	−98.21	−43.25	−39.32	−55.89	38.29	33.08	21.19	−1.70
1.5	−105.89	−44.47	−40.24	−48.02	35.13	26.34	19.79	−1.52
2	−108.10	−45.402	−40.97	−37.97	32.02	22.01	17.10	−1.02
2.5	−108.88	−45.73	−41.97	−30.93	28.89	17.98	16.77	−0.89
3	−109.29	−46.12	−42.53	−24.43	24.80	14.04	15.12	−0.78
3.5	−109.35	−45.93	−41.55	−19.89	22.08	11.35	13.29	−0.69
4	−109.29	−45.81	−41.53	−14.05	20.30	9.44	11.98	−0.51
4.5	−109.04	−45.50	−41.44	−11.23	19.19	8.41	10.13	−0.38
5	−108.92	−45.75	−41.39	−8.09	18.09	7.75	9.48	−0.32
5.5	−108.71	−44.96	−40.91	−5.48	18.25	7.48	6.32	−0.28
6	−108.32	−44.49	−40.76	−4.01	17.98	7.25	4.01	−0.26

ORCID iDs

Józef Spałek https://orcid.org/0000-0003-3867-8493

References

[1] Piela L 2013 *Ideas of Quantum Chemistry* 2nd edn (Amsterdam: Elsevier)

[2] Pauling L 1960 *The Nature of the Chemical Bond and the Structure of Molecules and Crystals: An Introduction to Modern Structural Chemistry* (*George Fisher Baker Non Resident Lecture Series*) (Ithaca, NY: Cornell University Press)

[3] Seitz F 1940 *The Modern Theory of Solids* (*International Series in Physics*) (New York: McGraw-Hill)

[4] Szabo A and Ostllund N S (ed) 1989 *Modern Quantum Chemistry: Introduction to Advanced Electronic Structure Theory* 2nd edn (New York: Dover)

[5] Gimarc B M 1979 *Molecular Structure and Bonding: The Qualitative Molecular Orbital Approach* (New York: Academic)

[6] Cooper D 2002 *Valence Bond Theory* (Amsterdam: Elsevier)

[7] Spałek J *et al* 2000 Optimization of single-particle basis for exactly soluble models of correlated electrons *Phys. Rev.* B **61** 15676–87

[8] Rycerz A and Spałek J 2001 Exact diagonalization of many-fermion Hamiltonian with wave-function renormalization *Phys. Rev.* B **63** 073101

[9] Spałek J *et al* 2007 The combined exact diagonalization *ab initio* approach and its application to correlated electronic states and Mott–Hubbard localization in nanoscopic systems *J. Phys.: Condens. Matter* **19** 255212

[10] Biborski A, Kądzielawa A P and Spałek J 2015 Combined shared and distributed memory *ab initio* computations of molecular-hydrogen systems in the correlated state: process pool solution and two-level parallelism *Comput. Phys. Commun.* **197** 7–16

[11] Biborski A, Kądzielawa A P and Spałek J 2017 Metallization of solid molecular hydrogen in two dimensions: Mott–Hubbard-type transition *Phys. Rev.* B **96** 085101

[12] Biborski A, Kądzielawa A P and Spałek J 2018 Atomization of correlated molecular-hydrogen chain: a fully microscopic variational Monte Carlo solution *Phys. Rev.* B **98** 085112

[13] Spalek J, Datta A and Honig J M 1987 Discontinuous metal–insulator transitions and Fermi-liquid behavior of correlated electrons *Phys. Rev. Lett.* **59** 728–31

[14] Phillips P 2011 Mottness collapse and T-linear resistivity in cuprate superconductors *Phil. Trans. R. Soc.* A **369** 1574–98

[15] Robertson B 1973 Introduction to field operators in quantum mechanics *Am. J. Phys.* **41** 678

[16] Jansen M and Wedig U 2008 A piece of the picture-misunderstanding of chemical concepts *Angew. Chem., Int. Ed.* **47** 10026–9

[17] Walsh A, Sokol A A, Buckeridge J, Scanlon D O and Catlow C R A 2018 Oxidation states and ionicity *Nat. Mater.* **17** 958–64

[18] Fugel M *et al* 2018 Covalency and ionicity do not oppose each other-relationship between Si–O bond character and basicity of siloxanes *Chem. Eur. J.* **24** 15275–86

[19] Martín Pendás A and Francisco E 2018 Decoding real space bonding descriptors in valence bond language *Phys. Chem. Chem. Phys.* **20** 12368–72

[20] Mott N 1991 *Metal–Insulator Transitions* 2nd edn (London: Taylor and Francis)

[21] Spalek J, Oleá A M and Chao K A 1981 Magnetic phases of strongly correlated electrons in a nearly half-filled narrow band *Phys. Status Solidi b* **108** 329
[22] Spałek J, Oleś A M and Honig J M 1983 Metal–insulator transition and local moments in a narrow band: a simple thermodynamic theory *Phys. Rev.* B **28** 6802–11
[23] Harris A B and Lange R V 1977 Single-particle excitations in narrow energy bands *J. Phys.* C **10** L271
[24] Harris A B, Lange R V and Oleś A M 1967 Single-particle excitations in narrow energy bands *Phys. Rev.* **157** 295–314
[25] Chandra A K and Sebastian K L 1976 A view of bond-formation in HeH^+ from the separated species *Mol. Phys.* **31** 1489–504
[26] Kołos W and Wolniewicz L 1964 Accurate adiabatic treatment of the ground state of the hydrogen molecule *J. Chem. Phys.* **41** 3663–73
[27] Wolniewicz L 1965 Variational treatment of the HeH^+ ion and the β-decay in HT *J. Chem. Phys.* **43** 1087–91
[28] Karo A M and Olson A R 1959 Configuration interaction in the lithium hydride molecule: I. A determinantal AO approach *J. Chem. Phys.* **30** 1232–40
[29] Pachucki K 2012 Born–Oppenheimer potential for HeH^+ *Phys. Rev.* A **85** 042511
[30] Limelette P, Georges A, Jeírome D, Wzietek P, Metcalf P and Honig J M 2003 Universality and critical behavior at the Mott transition *Science* **302** 89–92
[31] Spałek J 2020 Strongly correlated quantum matter: a subjective overview of selected fundamental aspects *Acta Phys. Polon.* B **51** 1147–84
[32] Spałek J unpublished.